Power-based control of physical systems

Garcia-Canseco, E.; Jeltsema, D.; Scherpen, J. M. A.; Ortega, R.

Published in:
IFAC Proceedings Volumes

Publication date:
2008

Proceedings of the 17th World Congress
The International Federation of Automatic Control
Seoul, Korea, July 6-11, 2008

Power–based control of physical systems: two case studies

Eloísa García–Canseco * **Dimitri Jeltsema** **
Jacquelien M.A. Scherpen * **Romeo Ortega** ***

* *Faculty of Mathematics and Natural Sciences, ITM, University of Groningen, Nijenborgh 4, 9747 AG Groningen, The Netherlands (e-mail: e.garcia.canseco{j.m.a.scherpen}@rug.nl)*

** *Delft Institute of Applied Mathematics, Delft University of Technology, Mekelweg 4, 2628 CD Delft, The Netherlands (e-mail: d.jeltsema@tudelft.nl)*

*** *Laboratoire des Signaux et Systèmes, SUPELEC, Plateau de Moulon, 91192, Gif-sur-Yvette, cedex, France (Tel: +33 1 69 85 17 60; e-mail: romeo.ortega@lss.supelec.fr)*

Abstract: It is well known that energy–balancing control is stymied by the presence of pervasive dissipation. To overcome this problem in electrical circuits, the alternative paradigm of power–shaping control was introduced in (Ortega et al., 2003)—where, as suggested by its name, stabilization is achieved shaping a function akin to power instead of the energy function. In a previous work (García-Canseco et al., 2006) we have extended this technique to general nonlinear systems. The method relies on the solution of a PDE, which identifies the open–loop storage function. Despite the intrinsic difficulty of solving PDEs, we show through some physical examples, that the power–shaping methodology yields storage functions corresponding to the power of the system. To motivate the application of this control technique beyond the realm of electrical circuits, we illustrate the procedure with two case studies: a micro–electromechanical system and a two–tank system.

Keywords: Passivity–based control, nonlinear control, stability, nonlinear systems

1. INTRODUCTION

The main idea behind passivity–based control, is to shape the open–loop storage function of the system, such that the closed–loop system energy function has a minimum at the desired equilibrium point. Within the so–called *energy–balancing control* methodology (Ortega et al., 2001, 2002; van der Schaft, 2000), the closed–loop energy function is the difference between the total (open–loop) energy function of the system and the energy supplied by the controller. Hence the name energy–balancing.

Unfortunately, as shown in (Ortega et al., 2001), energy–balancing control is stymied by the existence of pervasive dissipation—a term which refers to the existence of resistive elements whose power dissipation does not vanish at the desired equilibrium point. This is indeed the case in regulation of mechanical systems where the extracted power is the product of force and velocity and we want to drive the velocity to zero. Unfortunately, it is no longer the case for most electrical or electromechanical systems where power involves the product of voltages and currents and the latter may be nonzero for nonzero equilibria.

Several control methodologies have been developed to overcome the so–called *dissipation obstacle*, such as interconnection and damping assignment passivity–based control (IDA–PBC) (Ortega et al., 2002), where the stabilization problem is accomplished by endowing the closed–loop system with a desired port–Hamiltonian structure. In (Maschke et al., 2000), the authors derive a constructive procedure to generate new storage functions for nonzero equilibria in the presence of pervasive dissipation, by modifying the interconnection structure of the closed–loop for port–Hamiltonian systems with constant input control. Additionally, (Jeltsema et al., 2004) propose an alternative definition of the supply energy for port–Hamiltonian systems when the damping is pervasive, and the energy–balancing property is obtained via a swap of the damping terms. In (Ortega et al., 2007), some extensions of the control by interconnection methodology have been recently introduced to circumvent the dissipation obstacle.

In this paper, we concentrate on the paradigm of *power–shaping control*, as originally introduced in (Ortega et al., 2003) to overcome the dissipation obstacle in nonlinear RLC circuits. As suggested by its name, stabilization is achieved by shaping the power instead of the energy as is done in the aforementioned methodologies. The present work is a sequel of our previous developments (García-Canseco et al., 2006), where we have extended the power–shaping methodology to general nonlinear systems, and we have applied it to the stabilization problem of the benchmark tunnel diode circuit. To encourage the

application of power–shaping control beyond the realm of electrical circuits, we present two case studies that include the set point regulation problem of a micro–electromechanical system and a two–tank system.

Notation: All vectors defined in the paper are column vectors, including the gradient of a scalar function that we denote by the operator $\nabla = (\partial/\partial \boldsymbol{x})^\top$. Differentiation of functions with scalar arguments is denoted by $(\cdot)'$.

2. POWER–SHAPING CONTROL

The main result of (García-Canseco et al., 2006), which we state without proof, is contained in the following proposition.

Proposition 1. Consider the general nonlinear system

$$\dot{\boldsymbol{x}} = \boldsymbol{f}(\boldsymbol{x}) + \boldsymbol{g}(\boldsymbol{x})\boldsymbol{u}, \tag{1a}$$

$$\boldsymbol{y} = \boldsymbol{h}(\boldsymbol{x}), \tag{1b}$$

where $\boldsymbol{x} \in \mathbb{R}^n$, and $\boldsymbol{u}, \boldsymbol{y} \in \mathbb{R}^m$ are the input and output vectors, respectively. Assume

A.1 There exist a matrix $\mathbf{Q} : \mathbb{R}^n \to \mathbb{R}^{n\times n}$, $|\mathbf{Q}(\boldsymbol{x})| \neq 0$, that
  i) solves the partial differential equation
  $$\nabla(\mathbf{Q}(\boldsymbol{x})\boldsymbol{f}(\boldsymbol{x})) = [\nabla(\mathbf{Q}(\boldsymbol{x})\boldsymbol{f}(\boldsymbol{x}))]^\top, \tag{2}$$
  ii) and verifies $\mathbf{Q}(\boldsymbol{x}) + \mathbf{Q}^\top(\boldsymbol{x}) \preceq 0$.

A.2 There exist a scalar function $P_a : \mathbb{R}^n \to \mathbb{R}$ verifying
  iii)
  $$\boldsymbol{g}^\perp(\boldsymbol{x})\mathbf{Q}^{-1}(\boldsymbol{x})\nabla P_a(\boldsymbol{x}) = 0,$$
  where $\boldsymbol{g}^\perp(\boldsymbol{x})$ is a full–rank left annihilator of $\boldsymbol{g}(\boldsymbol{x})$,[1] and
  iv) $\boldsymbol{x}^\star = \arg\min P_d(\boldsymbol{x})$, where
  $$P_d(\boldsymbol{x}) := \int [\mathbf{Q}(\boldsymbol{x})\boldsymbol{f}(\boldsymbol{x})]^\top \mathrm{d}\boldsymbol{x} + P_a(\boldsymbol{x}). \tag{3}$$

Under these conditions, the control law

$$\boldsymbol{u} = \left[\boldsymbol{g}^\top(\boldsymbol{x})\mathbf{Q}^\top(\boldsymbol{x})\mathbf{Q}(\boldsymbol{x})\boldsymbol{g}(\boldsymbol{x})\right]^{-1}\boldsymbol{g}^\top(\boldsymbol{x})\mathbf{Q}^\top(\boldsymbol{x})\nabla P_a(\boldsymbol{x}) \tag{4}$$

ensures $\boldsymbol{x}^\star$ is a (locally) stable equilibrium with Lyapunov function $P_d(\boldsymbol{x})$. Assume, in addition,

A.3 $\boldsymbol{x}^\star$ is an isolated minimum of $P_d(\boldsymbol{x})$ and the largest invariant set contained in the set $\{\boldsymbol{x} \in \mathbb{R}^n | \nabla^\top P_d(\boldsymbol{x}) \left[\mathbf{Q}^{-1}(\boldsymbol{x}) + \mathbf{Q}^{-\top}(\boldsymbol{x})\right] \nabla P_d(\boldsymbol{x}) = 0\}$ equals $\{\boldsymbol{x}^\star\}$.

Then, the equilibrium $\boldsymbol{x}^\star$ is (locally) asymptotically stable and an estimate of its domain of attraction is given by the largest bounded level set $\{\boldsymbol{x} \in \mathbb{R}^n \mid P_d(\boldsymbol{x}) \leq c\}$.

Remark 1. Invoking Poincare's lemma, we observe that (2) is *equivalent* to the existence of a *potential function* $P : \mathbb{R}^n \to \mathbb{R}$ such that

$$\mathbf{Q}(\boldsymbol{x})\boldsymbol{f}(\boldsymbol{x}) = \nabla P(\boldsymbol{x}). \tag{5}$$

Substituting (1) in (5) and taking into account the full–rank property of $\mathbf{Q}(\boldsymbol{x})$ in A.1, we get

$$\mathbf{Q}(\boldsymbol{x})\dot{\boldsymbol{x}} = \nabla P(\boldsymbol{x}) + \mathbf{G}(\boldsymbol{x})\boldsymbol{u}, \tag{6}$$

where $\mathbf{G}(\boldsymbol{x}) := \mathbf{Q}(\boldsymbol{x})\boldsymbol{g}(\boldsymbol{x})$. In the context of RLC circuits, the form of (6) is due to Brayton and Moser (1964), and is precisely the starting point of power–shaping control (Ortega et al., 2003). In the same context, $\mathbf{Q} : \mathbb{R}^n \to \mathbb{R}^{n\times n}$ represents a *full rank* matrix containing the incremental inductance and capacitance matrices and $P : \mathbb{R}^n \to \mathbb{R}$ is the circuit's *mixed–potential function*, which has units of *power*, see (Ortega et al., 2003; Jeltsema, 2005) for further details. A practical advantage of the Brayton–Moser equations is that they naturally describe the dynamics of the system in terms of "easily" measurable quantities, that is, the inductor currents and capacitor voltages, instead of fluxes and charges that are normally used as canonical coordinates in port-Hamiltonian systems. See for instance (Jeltsema and Scherpen, 2004, 2007b), where some results in power converters have been derived using this framework.

[1] That is, $\boldsymbol{g}^\perp(\boldsymbol{x})\boldsymbol{g}(\boldsymbol{x}) = 0$, and $\mathrm{rank}(\boldsymbol{g}^\perp(\boldsymbol{x})) = n - m$

Remark 2. Assumption A.1 of Proposition 1 involves the solution of the PDE (2) subject to the sign constraint ii)—which may be difficult to satisfy. In (Ortega et al., 2003), a more constructive procedure is proposed to, starting from a pair $\{\mathbf{Q}, P\}$ describing the dynamics (6), explicitly generate alternative pairs $\{\widetilde{\mathbf{Q}}, \widetilde{P}\}$ that also describe the dynamics, i.e.,

$$\widetilde{\mathbf{Q}}(\boldsymbol{x})\dot{\boldsymbol{x}} = \nabla\widetilde{P}(\boldsymbol{x}) + \widetilde{\mathbf{G}}(\boldsymbol{x})\boldsymbol{u}, \tag{7}$$

where $\widetilde{\mathbf{G}}(\boldsymbol{x}) = \widetilde{\mathbf{Q}}(\boldsymbol{x})\boldsymbol{g}(\boldsymbol{x})$. For ease of reference in the sequel, we repeat here this result adapting the notation to the present context.

Proposition 2. (Ortega et al., 2003) Let $\mathbf{Q}(\boldsymbol{x})$ be an invertible matrix solution of (2) and define the full–rank matrix

$$\widetilde{\mathbf{Q}}(\boldsymbol{x}) := \left[\frac{1}{2}\nabla\left[\mathbf{Q}(\boldsymbol{x})\boldsymbol{f}(\boldsymbol{x})\right]\mathbf{M}(\boldsymbol{x}) + \frac{1}{2}\nabla^\top\left[\mathbf{M}(\boldsymbol{x})\mathbf{Q}(\boldsymbol{x})\boldsymbol{f}(\boldsymbol{x})\right] + \lambda\mathbf{I}\right]\mathbf{Q}(\boldsymbol{x}),$$

where $\lambda \in \mathbb{R}$ and $\mathbf{M} : \mathbb{R}^n \to \mathbb{R}^{n\times n}$, with $\mathbf{M} = \mathbf{M}^\top$, can be arbitrarily chosen. Then, the system (6) is equivalently described by (7), with

$$\widetilde{P}(\boldsymbol{x}) := \lambda\int\left[\mathbf{Q}(\boldsymbol{x})\boldsymbol{f}(\boldsymbol{x})\right]^\top d\boldsymbol{x} + \frac{1}{2}\boldsymbol{f}^\top(\boldsymbol{x})\mathbf{Q}^\top(\boldsymbol{x})\mathbf{M}(\boldsymbol{x})\mathbf{Q}(\boldsymbol{x})\boldsymbol{f}(\boldsymbol{x}).$$

Remark 3. Clearly, the power–shaping stage of the procedure—after transforming (1) into the form (6)—coincides with the one proposed in (Ortega et al., 2002) for energy–shaping using interconnection and damping assignment passivity–based control (IDA–PBC). Additional remarks on the relation between these techniques may be found in (Jeltsema, 2005; Blankenstein, 2005) and in the recent work (Ortega et al., 2007). Indeed, for port–Hamiltonian (pH) systems (van der Schaft, 2000)

$$\dot{\boldsymbol{x}} = [\mathbf{J}(\boldsymbol{x}) - \mathbf{R}(\boldsymbol{x})]\nabla H(\boldsymbol{x}) + \boldsymbol{g}(\boldsymbol{x})\boldsymbol{u}, \tag{8a}$$

$$\boldsymbol{y} = \boldsymbol{g}^\top(\boldsymbol{x})\nabla H(\boldsymbol{x}), \tag{8b}$$

with *full–rank* matrix $\mathbf{J}(\boldsymbol{x}) - \mathbf{R}(\boldsymbol{x})$, a trivial solution of (2) is obtained by setting $\mathbf{Q}(\boldsymbol{x}) = [\mathbf{J}(\boldsymbol{x}) - \mathbf{R}(\boldsymbol{x})]^{-1}$. However, in such case the associated potential function is not modified and remains the total stored energy instead of power as is desired.

The purpose of the next two sections is to illustrate the application of the power–shaping methodology of Proposition 1 using two well-known examples.

3. CASE STUDY I: A MICRO–ELECTROMECHANICAL SYSTEM

3.1 The Model

Consider the micro–electromechanical system depicted in Figure 1. The dynamical equations of motion are given by (Maithripala et al., 2005) (see also (van der Schaft, 2000)).

$$\dot{x}_1 = \frac{x_2}{m} \tag{9a}$$

$$\dot{x}_2 = -k(x_1 - x_{1_{\text{nom}}}) - \frac{b}{m}x_2 - \frac{x_3^2}{2A\epsilon} \tag{9b}$$

$$\dot{x}_3 = -\frac{x_1 x_3}{RA\epsilon} + \frac{1}{R}u, \tag{9c}$$

where the state vector $\boldsymbol{x} = [x_1\ x_2\ x_3]^\top$ consist of the air gap x_1 (with $x_{1_{\text{nom}}}$ the nominal value or zero voltage gap), the momentum x_2, and the charge of the device x_3. The plate area, the mass of the plate and the permittivity in the gap are represented by A, m, and ϵ, respectively. The spring and friction coefficients are given respectively by the positive constants k and b. The electrical input resistance is denoted by R and u represents the input voltage which is the control action. As pointed out in (Maithripala et al., 2005), x_2 is usually not available for measurement.

The assignable equilibria of the system are determined by $\boldsymbol{x}^\star = [x_1^\star\ 0\ x_3^\star]^\top$ where

$$(x_3^\star)^2 = -2kA\epsilon(x_1^\star - x_{1_{\text{nom}}}).$$

The corresponding constant control is given by

$$u^\star = \frac{x_1^\star x_3^\star}{A\epsilon}.$$

3.2 Controller Design

The control objective is to stabilize any constant desired air gap position $x_1^\star$. Following the power–shaping procedure outlined in Section 2, we have the following result.

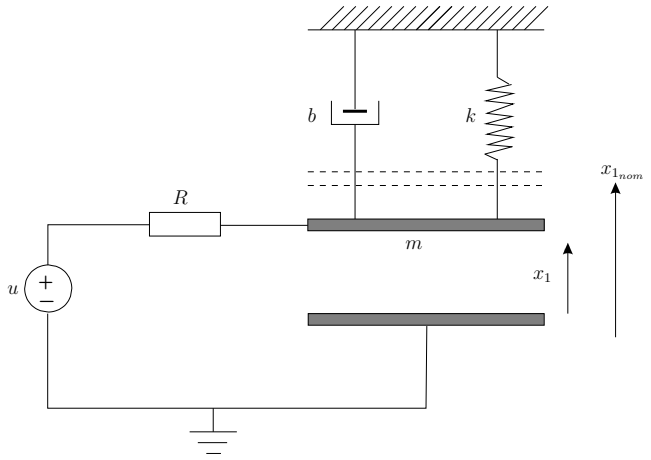

Fig. 1. Model of an electrostatic microactuator.

Proposition 3. The dynamics of the micro–electromechani-cal system (9), in closed–loop with the controller

$$u = -\alpha_1(x_1 x_3 - x_1^\star x_3^\star) - \alpha_2(x_3 - x_3^\star) + u^\star, \tag{10}$$

has a locally asymptotically stable equilibrium point $\boldsymbol{x}^\star$ with Lyapunov function

$$\begin{aligned} P_d(\boldsymbol{x}) = &\frac{kx_2}{m}(x_1 - x_{1_{\text{nom}}}) + \frac{x_2 x_3^2}{2A\epsilon m} + \frac{bx_2^2}{2m^2} + \frac{x_1^2 x_3^2}{2RA^2\epsilon^2} \\ &+\frac{\lambda}{2}\left(k(x_1 - x_{1_{\text{nom}}})^2 + \frac{x_2^2}{m} + \frac{x_1 x_3^2}{A\epsilon}\right) - \frac{(u^\star)^2}{2\alpha_1 RA\epsilon} \\ &+\frac{\alpha_1}{2RA\epsilon}\left(x_1 x_3 - x_1^\star x_3^\star + \alpha_3(x_3 - x_3^\star) - \frac{u^\star}{\alpha_1}\right)^2, \end{aligned} \tag{11}$$

provided α_1 satisfies

$$\alpha_1 > \frac{k^2}{(x_3^\star)^2(b + \lambda m)} - \frac{(x_3^\star)^2 + kA\epsilon\alpha_3}{RA^2\epsilon^2(x_3^\star)^2},$$
$$A\epsilon(\alpha_3 + 3x_1^\star - 2x_{1_{\text{nom}}})\alpha_1 > 3x_1^\star - 2x_{1_{\text{nom}}}$$

and

$$\alpha_2 = \alpha_1\alpha_3, \quad \alpha_3 = \lambda RA\epsilon, \quad \lambda \in \{(\frac{k}{b}, \infty) \cap (-\frac{x_1^\star}{RA\epsilon}, \infty)\}.$$

Proof. Observe that the micro–electromechanical system (9) in pH form (8), with

$$\mathbf{J} - \mathbf{R} = \begin{bmatrix} 0 & 1 & 0 \\ -1 & -b & 0 \\ 0 & 0 & -1/R \end{bmatrix}, \quad \boldsymbol{g} = \begin{bmatrix} 0 \\ 0 \\ 1/R \end{bmatrix},$$

and the energy function

$$H(\boldsymbol{x}) = \frac{k}{2}(x_1 - x_{1_{\text{nom}}})^2 + \frac{x_2^2}{2m} + \frac{x_1 x_3^2}{2A\epsilon}. \tag{12}$$

Since the matrix $\mathbf{J} - \mathbf{R}$ is full–rank, a trivial solution of the PDE (2) is given by

$$\mathbf{Q} = [\mathbf{J} - \mathbf{R}]^{-1} = \begin{bmatrix} -b & -1 & 0 \\ 1 & 0 & 0 \\ 0 & 0 & -R \end{bmatrix}. \tag{13}$$

Hence, (9) can be written in the form (6) as

$$\mathbf{Q}\dot{\boldsymbol{x}} = \nabla P(\boldsymbol{x}) + \mathbf{G}u,$$

where $\mathbf{G} = [\mathbf{J} - \mathbf{R}]^{-1}\boldsymbol{g}$. Although (13) is negative semi-definite, the potential function still equals the original energy function given in (12), that is, $P(\boldsymbol{x}) = H(\boldsymbol{x})$, and not a power function as desired.

To proceed with the power–shaping methodology, we apply Proposition 2 to look for another pair $\{\widetilde{\mathbf{Q}}, \widetilde{P}\}$ that alternatively describes the dynamics (9), with $\tilde{P}$ a power–like function. It turns out that with the choice $\lambda > 0$ and

$$\lambda \in \{(\frac{k}{b}, \infty) \cap (-\frac{x_1^\star}{RA\epsilon}, \infty)\}, \quad \mathbf{M} = \begin{bmatrix} 0 & 1 & 0 \\ 1 & b & 0 \\ 0 & 0 & 1/R \end{bmatrix},$$

equations (9) can be rewritten as (7), with

$$\widetilde{\mathbf{Q}}(\boldsymbol{x}) = \begin{bmatrix} k - \lambda b & -\lambda & -\dfrac{x_3}{A\epsilon} \\ \lambda & -\dfrac{1}{m} & 0 \\ \dfrac{x_3}{A\epsilon} & 0 & -\dfrac{x_1}{A\epsilon} - \lambda R \end{bmatrix},$$

and

$$\tilde{\mathbf{G}} = \begin{bmatrix} -\dfrac{x_3}{RA\epsilon} \\ 0 \\ \dfrac{-x_1}{RA\epsilon} - \lambda \end{bmatrix}.$$

Notice that $\widetilde{\mathbf{Q}}(\boldsymbol{x})$ is locally negative semi–definite, i.e., $\widetilde{\mathbf{Q}}(\boldsymbol{x}) + \widetilde{\mathbf{Q}}^\top(\boldsymbol{x}) \preceq 0$ for all $\boldsymbol{x} \in \mathbb{R}^n$ such that $\|\boldsymbol{x} - \boldsymbol{x}^\star\|$ is sufficiently small. Moreover, the new mixed–potential function

$$\widetilde{P}(\boldsymbol{x}) = \frac{kx_2}{m}(x_1 - x_{1_{\text{nom}}}) + \frac{x_2 x_3^2}{2A\epsilon m} + \frac{bx_2^2}{2m^2} + \frac{x_1^2 x_3^2}{2RA^2\epsilon^2} + \lambda H(\boldsymbol{x}) \tag{14}$$

is a power–like function. Indeed, since $x_2/m =: v_m$ (velocity of the mass), $x_3^2/(2A\epsilon) =: f_e$ (force of electrical origin), $k(x_1 - x_{1_{\text{nom}}}) =: f_k$ (force of the spring), $x_1 x_3/(A\epsilon) := u_c$ (voltage across the capacitor), and $1/\lambda =: \tau$ has units of seconds, thus (14) can be recast into

$$\widetilde{P}(\cdot) = \frac{b}{2}v_m^2 + f_k v_m + f_e v_m + \frac{u_c^2}{2R} + \frac{H}{\tau}.$$

Clearly, the first term represents the mechanical resistive content, whereas the second and third term exhibit the product force × velocity, and the fourth term represents the electrical resistive co–content. The last term is elucidated recalling that energy per second equals power.

Furthermore, the selection

$$\widetilde{\mathbf{G}}^\perp(\boldsymbol{x}) = \begin{bmatrix} -x1 - \lambda RA\epsilon & -1 + \lambda x_1 + \lambda^2 RA\epsilon & x_3 \\ 0 & -1 & 0 \end{bmatrix}$$

yields that condition iii) of Proposition 1, $\widetilde{\mathbf{G}}^\perp(\boldsymbol{x})\nabla P_a = 0$, becomes the following PDEs

$$-(x1 + \lambda RA\epsilon)\frac{\partial P_a}{\partial x_1} + (\lambda x_1 + \lambda^2 RA - 1)\frac{\partial P_a}{\partial x_2} + x_3\frac{\partial P_a}{\partial x_3} = 0,$$
$$\frac{\partial P_a}{\partial x_2} = 0,$$

whose solution has the form

$$P_a(\boldsymbol{x}) = \Psi(x_3(x_1 + \lambda RA\epsilon)).$$

The function $\Psi(\cdot)$ must be chosen so that $P_d(\boldsymbol{x}) = \widetilde{P}(\boldsymbol{x}) + P_a(\boldsymbol{x})$ satisfies the equilibrium assignment and stability conditions of Proposition 1, that is, $P_d(\boldsymbol{x})$ should verify $\nabla P_d(\boldsymbol{x}^\star) = 0$ and $\nabla^2 P_d(\boldsymbol{x}^\star) \succ 0$. A suitable selection of $\Psi(\cdot)$ is given by

$$\Psi(z(x_1, x_3)) = \frac{1}{2}\kappa(z - z^\star)^2 + \mu(z - z^\star),$$

where $z = x_3(x_1 + \alpha_3)$, $z^\star = x_3^\star(x_1^\star + \alpha_3)$, and $\alpha_3 = \lambda RA\epsilon$. The equilibrium is assigned with $\mu = -\frac{u^\star}{RA\epsilon}$. Now, the Hessian of $P_d(\boldsymbol{x})$ is calculated as

$$\nabla^2 P_d(\boldsymbol{x})\big|_{\boldsymbol{x}=\boldsymbol{x}^\star} = \begin{bmatrix} \lambda k + \left(\kappa + \dfrac{1}{RA^2\epsilon^2}\right)(x_3^\star)^2 & \dfrac{k}{m} & \dfrac{x_3^\star(x_1^\star + \alpha_3)(\kappa RA^2\epsilon^2 + 1)}{RA^2\epsilon^2} \\ \dfrac{k}{m} & \dfrac{b + \lambda m}{m^2} & \dfrac{x_3^\star}{mA\epsilon} \\ \dfrac{x_3^\star(x_1^\star + \alpha_3)(\kappa RA^2\epsilon^2 + 1)}{RA^2\epsilon^2} & \dfrac{x_3^\star}{mA\epsilon} & \dfrac{(x_1^\star)^2}{RA^2\epsilon^2} + \dfrac{\lambda x_1^\star}{A\epsilon} + \kappa(x_1^\star + \alpha_3) \end{bmatrix}.$$

Some computations show that $\nabla^2 P_d(\boldsymbol{x}^\star) \succ 0$ if and only if $\kappa > 0$ satisfies the following inequalities

$$\kappa > \frac{RA\epsilon k^2}{(x_3^\star)^2(b + \lambda m)} - \frac{(x_3^\star)^2 + kA\epsilon\alpha_3}{A\epsilon(x_3^\star)^2},$$
$$RA^2\epsilon^2(\alpha_3 + 3x_1^\star - 2x_{1_{\text{nom}}})\kappa > 3x_1^\star - 2x_{1_{\text{nom}}}.$$

Finally, by using (4) and setting $\alpha_1 = RA\epsilon\kappa$, $\alpha_2 = \alpha_1\alpha_3$, yields the control law (10). Notice further that controller (10) does not depend on the unmeasurable coordinate x_2. ■

3.3 Simulation Results

Figures 2, 3, and 4 depict the level curves of the function P_d (11), where for simplicity, the model parameters R, m, k, b, A and ϵ have been set to one, and $x_{1_{\text{nom}}} = 0.4$. The gains were selected as $\lambda = 2$, $\alpha_1 = 3$. Observe that $\boldsymbol{x}^\star = [0.2\ 0\ 0.63]^\top$ is a local minimum point of P_d (11).

Figure 5 show the closed–loop behavior of the air gap position to a step change in $x_1^\star$ from 0.2 to 0. The initial conditions are $\boldsymbol{x}(0) = [0\ \ 0\ \ 0.5]^\top$. As can be seen, the control law (10) depicted in Figure 6, effectively stabilizes the system.

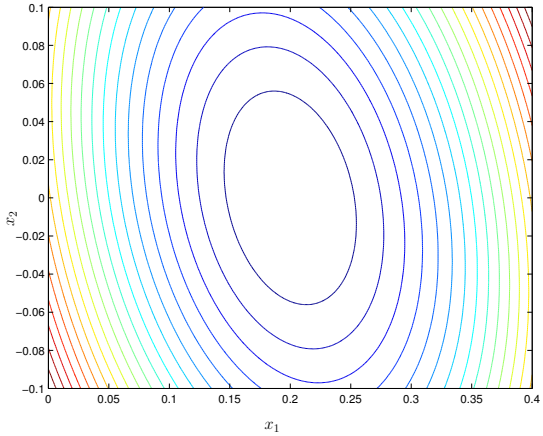

Fig. 2. Micro–electromechanical system: level curves in the plane (x_1, x_2) for $x_3 = x_3^\star = 0.63$.

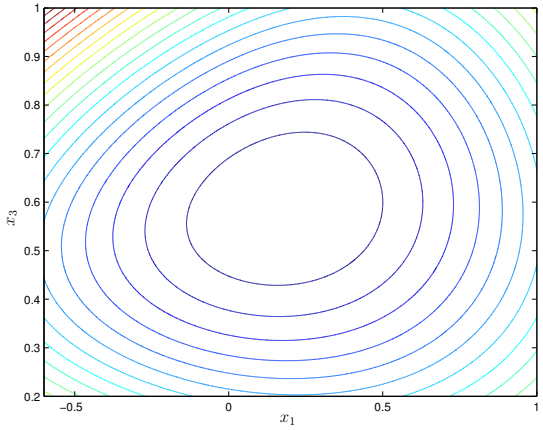

Fig. 3. Micro–electromechanical system: level curves in the plane (x_1, x_3) for $x_2 = x_2^\star = 0$.

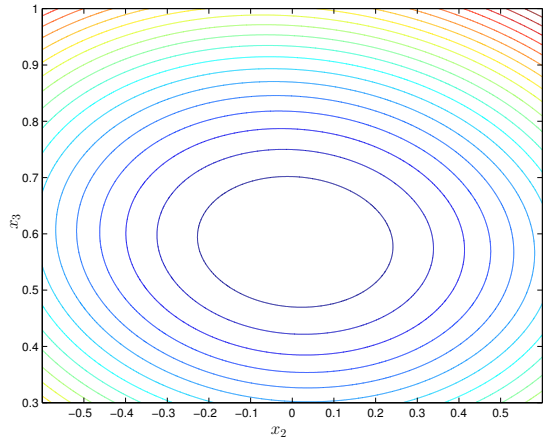

Fig. 4. Micro–electromechanical system: level curves in the plane (x_2, x_3) for $x_1 = x_1^\star = 0.2$.

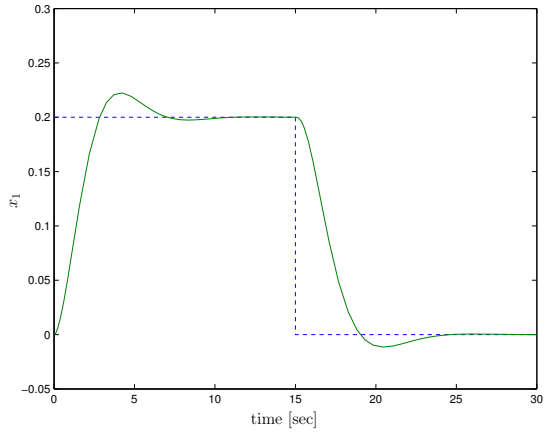

Fig. 5. Micro–electromechanical system: Air gap x_1

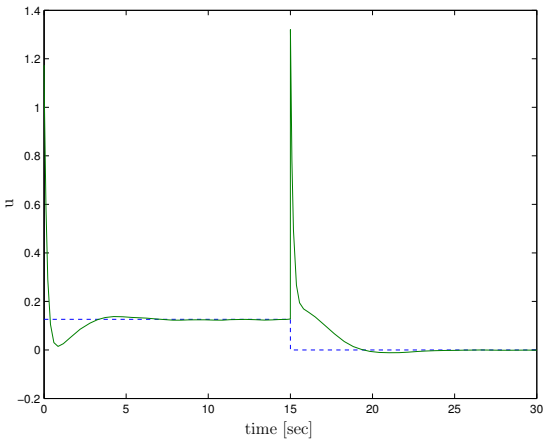

Fig. 6. Micro–electromechanical system: control law u (10).

4. CASE STUDY II: TWO–TANK SYSTEM

4.1 The Model

Consider the two–tank system depicted in Figure 7. Using Torricelli's law, the dynamics of the system can be written as (Johnsen and Allgower, 2006)

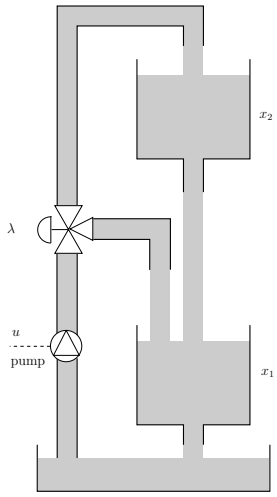

Fig. 7. Two–tank system.

$$\dot{x}_1 = -\frac{a_1\sqrt{2gx_1}}{A_1} + \frac{a_2\sqrt{2gx_2}}{A_1} + \frac{\gamma}{A_1}u \tag{15a}$$

$$\dot{x}_2 = -\frac{a_2\sqrt{2gx_2}}{A_2} + \frac{1-\gamma}{A_2}u, \tag{15b}$$

where the state variables $x_1 > 0$ and $x_2 > 0$ represent the water level in the lower and upper tank, respectively. The system parameters are all positive constants, where g is the gravitational constant and, A_i and a_i, with $i = 1, 2$, are the cross sections of the tanks and the outlet holes, respectively. The valve parameter is the constant $\gamma \in [0, 1]$, with $\gamma = 0$ if the valve is fully open, i.e., all the water is directed to the upper tank, and $\gamma = 1$ if the valve is closed.

The assignable equilibrium points of the system are determined by

$$x_1^\star = \frac{a_2^2}{a_1^2(\gamma-1)^2}x_2^\star,$$

with the corresponding constant control

$$u^\star = \frac{a_2\sqrt{2gx_2^\star}}{1-\gamma},$$

for all $\gamma \in [0, 1)$, and by $x_2^\star = 0$, $u^\star = a_1\sqrt{2gx_1^\star}$ for $\gamma = 1$.

4.2 Controller Design.

The control objective is to stabilize a given equilibrium point $\boldsymbol{x}^\star = [x_1^\star\ x_2^\star]^\top$. Following the power-shaping procedure outlined in Section 1, we have the following result.

Proposition 4. Consider the two–tank system (15) in closed–loop with the linear state feedback controller

$$u = -k_1(x_1 - x_1^\star) - k_2(x_2 - x_2^\star) + u^\star. \tag{16}$$

If the tuning parameters k_1 and k_2 satisfy

$$k_1 > 0, \quad k_2 > \frac{(1-\gamma)A_2}{4A_1}k_1, \tag{17}$$

then $\boldsymbol{x}$ is a globally asymptotically stable equilibrium of the closed–loop system with Lyapunov function

$$P_d(\boldsymbol{x}) = \frac{2a_1k_1\sqrt{2g}}{3A_1}x_1^{\frac{3}{2}} + \frac{2a_2k_2\sqrt{2g}}{3(1-\gamma)A_1}x_2^{\frac{3}{2}} \tag{18}$$
$$+ \frac{1}{2A_1}\left[k_1(x_1 - x_1^\star) + k_2(x_2 - x_2^\star) - u^\star\right]^2 + \frac{(u^\star)^2}{2A_1}.$$

Proof. Fixing the matrix $\mathbf{Q}$ constant, i.e., $\mathbf{Q} = \{q_{ij}\}$, with $i, j = 1, 2$, a suitable solution to the PDE (2) yields

$$q_{11} < 0, \quad q_{12} = \frac{A_2 q_{11}}{A_1}, \quad q_{21} = 0, \quad q_{22} < 0. \tag{19}$$

Hence, $\mathbf{Q}$ is invertible and under Assumption A.4 verifies $\mathbf{Q} + \mathbf{Q}^\top \preceq 0$ if and only if $q_{22} > \frac{A_2^2 q_{11}}{4A_1^2}$.

To simplify the computations, let

$$q_{11} = -k_1, \quad q_{22} = -\frac{A_2 k_2}{A_1(1-\gamma)},$$

where k_1 and k_2 are positive constants. Consequently, the condition to make the symmetric part of the matrix $\mathbf{Q}$ negative semi–definite becomes (17). Moreover, the mixed–potential function

$$P(\boldsymbol{x}) = \frac{2a_1 k_1 \sqrt{2g}}{3A_1} x_1^{\frac{3}{2}} + \frac{2a_2 k_2 \sqrt{2g}}{3(1-\gamma)A_1} x_2^{\frac{3}{2}}, \tag{20}$$

can be seen as a power–like function. Indeed, by Torricelli's law, we know that the terms $\sqrt{2gx_1}$ and $\sqrt{2gx_2}$ have the units of velocity, hence we define $v_1 := \sqrt{2gx_1}$ and $v_2 := \sqrt{2gx_2}$. Furthermore, by fixing the units of k_1 and k_2 to kg/s^2 so that the terms $k_1 x_1 =: f_1$ and $k_2 x_2 =: f_2$ have units of force, and defining the unitless constants $\beta_1 = \frac{2a_1}{3A_1}$, $\beta_2 = \frac{2a_2}{3(1-\gamma)A_2}$, the mixed–potential function (20) can be recast into

$$P(\cdot) = \beta_1 f_1 v_1 + \beta_2 f_2 v_2,$$

which clearly exhibits the products force $\times$ velocity. Furthermore, by choosing

$$\boldsymbol{g}^\perp = \begin{bmatrix} -\dfrac{1-\gamma}{A_2} & \dfrac{\gamma}{A_1} \end{bmatrix},$$

condition iii) of Proposition 1 becomes

$$\frac{1}{k_1}\frac{\partial P_a}{\partial x_1} - \frac{1}{k_2}\frac{\partial P_a}{\partial x_2} = 0. \tag{21}$$

The solution of (21) yields $P_a(\boldsymbol{x}) = \Psi(\frac{k_1}{k_2}x_1 + x_2)$, where $\Psi(\cdot)$ is an arbitrary differentiable function that must be chosen so that $P_d(\boldsymbol{x}) = P(\boldsymbol{x}) + P_a(\boldsymbol{x})$ has a minimum at $\boldsymbol{x}^\star$. Computing $P_d(\boldsymbol{x})$ from (3), we obtain

$$P_d(\boldsymbol{x}) = \frac{2a_1 k_1 \sqrt{2g}}{3A_1} x_1^{\frac{3}{2}} + \frac{2a_2 k_2 \sqrt{2g}}{3(1-\gamma)A_1} x_2^{\frac{3}{2}} + \Psi\left(\frac{k_1}{k_2}x_1 + x_2\right),$$

which should satisfy $\nabla P_d(\boldsymbol{x}^\star) = 0$ and $\nabla^2 P_d(\boldsymbol{x}^\star) \succ 0$. As in the previous example, one possibility is to select a quadratic function of the form

$$\Psi(z(\boldsymbol{x})) = \frac{\kappa}{2}(z - z^\star)^2 + \mu(z - z^\star),$$

where $z = \frac{k_1}{k_2}x_1 + x_2$, $z^\star = z(\boldsymbol{x}^\star)$, $\kappa > 0$, and μ are scalars. Some simple calculations show that the minimum is assigned, i.e., $\nabla P_d(\boldsymbol{x}^\star) = 0$, if we set $\mu = -\frac{k_2 u^\star}{A_1}$. The Hessian $\nabla^2 P_d$ is calculated as

$$\nabla^2 P_d = \begin{bmatrix} \dfrac{k_1 a_1 \sqrt{2g}}{2A_1\sqrt{x_1}} + \dfrac{\kappa k_1^2}{k_2^2} & \dfrac{\kappa k_1}{k_2} \\ \dfrac{\kappa k_1}{k_2} & \dfrac{k_2 a_2 \sqrt{2g}}{2A_1(1-\gamma)\sqrt{x_2}} + \kappa \end{bmatrix},$$

which is positive definite for all positive $\boldsymbol{x}$. Setting $\kappa = \frac{k_2^2}{A_1}$ yields the Lyapunov function (18), which has a unique minimum at $\boldsymbol{x}^\star$. Finally, from (4) we obtain the simple linear state feedback (16), which asymptotically stabilizes the equilibrium point $\boldsymbol{x}^\star$, provided (17) holds. ■

Remark 4. The controller (16) was also derived using the IDA–PBC methodology in (Johnsen and Allgower, 2006). We refer to the aforementioned work for simulations and experimental results.

5. CONCLUSIONS AND FUTURE WORK

Two case studies illustrating the power–shaping methodology of general nonlinear systems, as recently proposed by (García-Canseco et al., 2006), are presented.

Among the issues that remain open and are currently being explored are the solvability of the PDE (2) for a general class of systems and other applications of power–shaping, for instance, to mechanical systems. Although some modeling issues based on the Brayton–Moser equations have been considered in (Jeltsema and Scherpen, 2007a), many control issues using this power–based framework still remain open.

REFERENCES

G. Blankenstein. Power balancing for a new class of nonlinear systems and stabilization of RLC circuits. *International Journal of Control*, 78(3):159–171, 2005.

R.K. Brayton and J.K. Moser. A theory of nonlinear networks-I. *Quart. of App. Math*, 22:1–33, April 1964.

E. García-Canseco, R. Ortega, J. M. A. Scherpen, and D. Jeltsema. Power shaping control of nonlinear systems: A benchmark example. In *3rd Workshop on Lagrangian and Hamiltonian Methods for Nonlinear Control*, Nagoya, Japan., July 19-21 2006.

D. Jeltsema. *Modeling and control of nonlinear networks: a power–based perspective.* PhD thesis, Delft University of Technology, The Netherlands, May 2005.

D. Jeltsema and J.M.A. Scherpen. A power–based description of standar mechanical systems. *Systems & Control Letters*, 56(5):349–356, May 2007a.

D. Jeltsema and J.M.A. Scherpen. Tuning of passivity–preserving controllers for switched–mode power converters. *IEEE Trans. on Automatic Control*, 49(8):1333–1344, August 2004.

D. Jeltsema and J.M.A. Scherpen. A power–based perspective in modeling and control of switched power converters (past and present). *IEEE Industrial Electronics Magazine*, 1(1):7,54, 2007b.

D. Jeltsema, R. Ortega, and J.M.A. Scherpen. An energy–balancing perspective of interconnection and damping assignment control of nonlinear systems. *Automatica*, 40(9):1643–1646, 2004.

J. Johnsen and F. Allgower. Interconnection and damping assignment passivity–based control of a four–tank system. In *3rd IFAC Workshop on Lagrangian and Hamiltonian Methods in Nonlinear Control*, Nagoya, Japan, July 19-22, 2006.

D. H. S. Maithripala, J. M. Berg, and W. P. Dayawansa. Control of an electrostatic mems using static and dynamic output feedback. *ASME Journal of Dynamical Systems Measurement and Control*, 127:443–450, 2005.

B. Maschke, R. Ortega, and A.J van der Schaft. Energy–based lyapunov functions for forced Hamiltonian sys-

tems with dissipation. *IEEE Trans. on Automatic Control*, 45(8):1498–1502, 2000.

R. Ortega, A.J. van der Schaft, I. Mareels, and B. Maschke. Putting energy back in control. *IEEE Control Systems Magazine*, 21(2):18–33, 2001.

R. Ortega, A.J. van der Schaft, B.M. Maschke, and G. Escobar. Interconnection and damping assignment passivity–based control of port–controlled Hamiltonian systems. *Automatica*, 38(4):585–596, 2002.

R. Ortega, D. Jeltsema, and J.M.A. Scherpen. Power shaping: a new paradigm for stabilization of nonlinear RLC circuits. *IEEE. Trans. on Automatic Control*, 48 (10):1762– 1767, October 2003.

R. Ortega, A. van der Schaft, F. Castaños, and A. Astolfi. Control by state–modulated interconnection of port–hamiltonian systems. In *7th IFAC Symposium on Nonlinear Control Systems (NOLCOS'07)*, Pretoria, South Africa, August 22-24, 2007.

A.J. van der Schaft. $\mathcal{L}_2$ *–Gain and passivity techniques in nonlinear control*. Springer–Verlag, 2000.